ORNL/TM--11545

DE91 010487

Fusion Energy Division

ATF EDGE PLASMA TURBULENCE STUDIES USING A FAST RECIPROCATING LANGMUIR PROBE

T. Uckan
C. Hidalgo*
J. D. Bell
J. H. Harris
J. L. Dunlap
G. R. Dyer
P. K. Mioduszewski
J. B. Wilgen

Ch. P. Ritz
A. J. Wootton
T. L. Rhodes
K. Carter
Fusion Research Center, The University of Texas, Austin

*Permanent address: Asociación EURATOM/CIEMAT, Madrid, Spain.

Date published: January 1991

Prepared for the
Office of Fusion Energy
under Budget Activity No. AT 10 10 15 B

Prepared by
OAK RIDGE NATIONAL LABORATORY
Oak Ridge, Tennessee 37831-6285
managed by
MARTIN MARIETTA ENERGY SYSTEMS, INC.
for the
U.S. DEPARTMENT OF ENERGY
under contract DE-AC05-84OR21400

CONTENTS

ABSTRACT

Electrostatic turbulence on the edge of the Advanced Toroidal Facility (ATF) torsatron is investigated experimentally with a fast reciprocating Langmuir probe (FRLP) array. Initial measurements of plasma electron density n_e and temperature T_e and fluctuations in density ($\tilde{n}_e$) and plasma floating potential ($\tilde{\phi}_f$) are made in electron cyclotron heated plasmas at 1 T. At the last closed flux surface (LCFS, $r/\bar{a} \sim 1$), $T_e \approx$ 20–40 eV and $n_e \approx 10^{12}$ cm^{-3} for a line-averaged electron density $\bar{n}_e = (3\text{–}6) \times 10^{12}$ cm^{-3}. Relative fluctuation levels, as the FRLP is moved into core plasma where $T_e > 20$ eV, are $\tilde{n}_e/n_e \approx 5\%$ and $e\tilde{\phi}_f/T_e \approx 2\tilde{n}_e/n_e$ about 2 cm inside the LCFS. The observed fluctuation spectra are broadband (40–300 kHz) with $\bar{k}\rho_s \leq 0.1$, where $\bar{k}$ is the wavenumber of the fluctuations and ρ_s is the ion Larmor radius at the sound speed. The propagation direction of the fluctuations reverses to the electron diamagnetic direction around $r/\bar{a} < 1$. The phase velocity and the electron drift velocity are comparable ($v_{ph} \sim v_{de}$). The fluctuation-induced particle flux is comparable to fluxes estimated from the particle balance using the H_α spectroscopic measurements. Many of the features seen in these experiments resemble the features of ohmically heated plasmas in the Texas Experimental Tokamak (TEXT).

1. INTRODUCTION

Energy and particle confinement in tokamaks and stellarators is anomalous, and results from the two types of devices show similar dependences on plasma parameters [1]. The study of electrostatic fluctuations [2] in different magnetic configurations may help to identify the underlying physics mechanisms responsible for plasma transport. To investigate the effects of the magnetic configuration on the characteristics of edge turbulence, recent measurements of electrostatic fluctuations at the edge of the Texas Experimental Tokamak (TEXT) [3] have been extended to the Advanced Toroidal Facility (ATF) [4] torsatron. Experimental observations on TEXT indicate that electrostatic fluctuations are the dominant mechanism for energy and particle losses in the edge [3,5]. To understand the driving forces on the edge turbulence in terms of the plasma current and the magnetic configuration, initial edge fluctuation measurements have been carried out on the currentless ATF device with a diagnostic setup similar to that used in the TEXT experiments, that is, a fast reciprocating Langmuir probe (FRLP) array [6].

The FRLP has been used to characterize, from an experimental point of view, the electrostatic turbulence on the edge of the ATF torsatron. The experimental setup and the analysis method are described in Sect. 2. Measurements of plasma electron density n_e, electron temperature T_e, and fluctuations in density ($\tilde{n}_e$) and plasma floating potential ($\tilde{\phi}_f$) at the edge of electron cyclotron heated (ECH) plasmas in ATF are presented and their turbulence characteristics are discussed in Sect. 3. Brief conclusions follow in Sect. 4.

2. EXPERIMENTAL SETUP

The stellarator configuration of the ATF torsatron has a poloidal multipolarity l = 2, 12 field periods (M = 12), a major radius R_0 = 2.1 m, and an average plasma radius $\bar{a}$ = 0.27 m. The externally produced currentless magnetic configuration has moderate shear; that is, the central rotational transform ($\iota/2\pi$ = 1/q) of 0.3 becomes 1.0 at the last closed flux surface (LCFS). Initial fluctuation measurements in ATF were carried out around the LCFS with the FRLP in ECH plasmas at a magnetic field B = 1 T. Plasmas were created using a gyrotron source at 53 GHz with heating power P = 200 kW. In these ECH plasmas, a representative range for the line-averaged plasma density is $\bar{n}_e$ = (3–6) × 10^{12} cm^{-3}, and the plasma stored energy $W_p \approx$ 1–2 kJ.

The FRLP is located one field period away from the instrumented rail limiter [7]. The probe is inserted into the edge plasma from the top, moves 5 cm into the plasma in 50 ms, and remains there about for 40 ms to carry out the fluctuation measurements. The FRLP head consists of a square array of four tips, 0.5 mm in diameter, that are 2 mm long and 2 mm apart. Double Langmuir probe operation of two tips, aligned perpendicular to the local magnetic field, makes it possible to measure the edge plasma n_e, T_e, and $\tilde{n}_e / n_e$ profiles inside (about 2 cm) and outside the LCFS, as indicated in Fig. 1. The other two tips are used to measure $\tilde{\phi}_f$ and the wavenumber k perpendicular to the local magnetic field. The data have been analysed using spectral analysis techniques [8]. That is, the fluctuation signals are digitized at 1 MHz, and fast Fourier transform (FFT) is

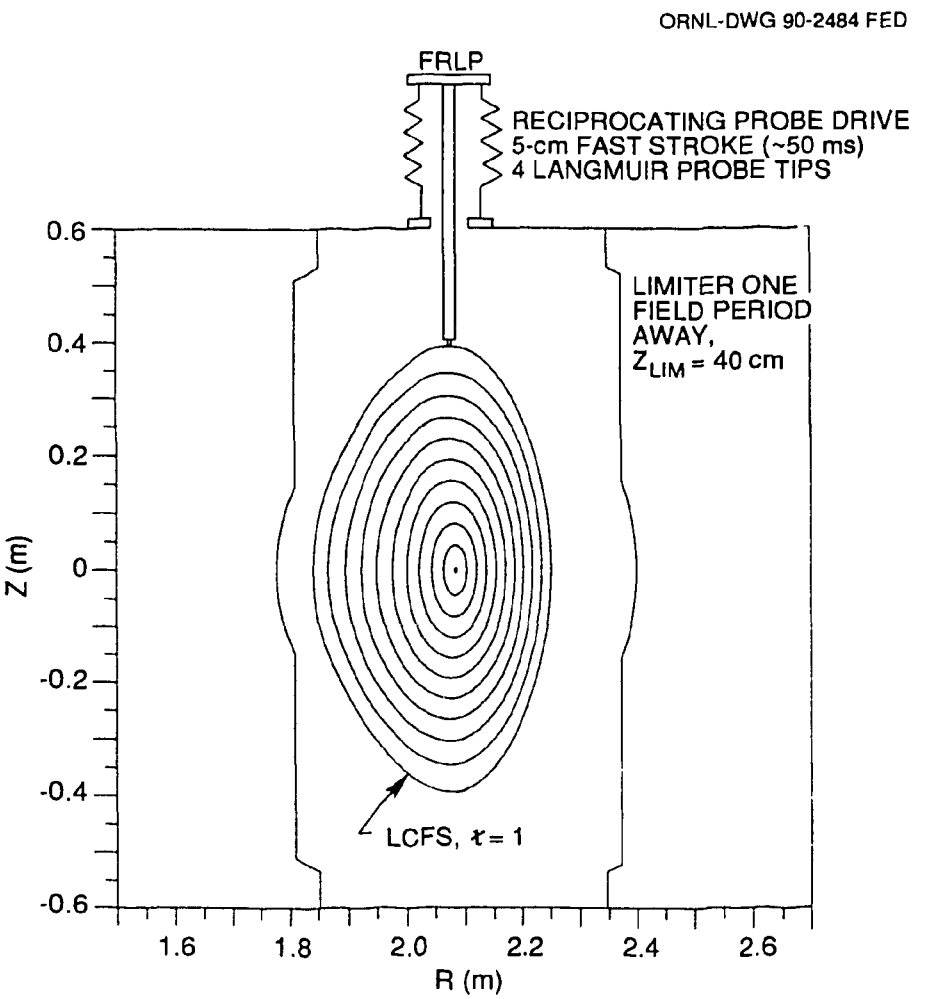

Fig. 1. Constant flux surfaces and the location of the FRLP on ATF.

used to obtain their power spectrum $S(k,\omega)$ as a function of frequency ω and k using the two-probe technique described in ref. [9]. Ensemble averaging of the spectral distribution of the flux $\tilde{\Gamma}(\omega)$, obtained from the correlation of density and plasma potential fluctuations ($\tilde{\phi}_p$), gives the turbulence-induced radial particle flux:

$$\tilde{\Gamma} = \langle \tilde{n}_e \tilde{v}_r \rangle = 2 \Sigma_{\omega>0} \tilde{\Gamma}(\omega). \tag{1}$$

Here $\tilde{v}_r = -ik\tilde{\phi}_p/B$ is the radial velocity due to the electrostatic fluctuations, and the frequency-resolved flux is estimated from many independent realizations using a triple correlation technique [10]:

$$\tilde{\Gamma}(\omega) = \mathrm{Re}[\langle -ik(\omega)\tilde{n}_e^*(\omega)\tilde{\phi}_p(\omega)\rangle]/B. \tag{2}$$

Further, to gain an insight into the physical process, $\tilde{\Gamma}(\omega)$ can be expressed as [8]

$$\tilde{\Gamma}(\omega) \approx (k/B)\gamma_{\tilde{n}\tilde{\phi}} n_{rms}\phi_{rms}\sin\theta_{\tilde{n}\tilde{\phi}}, \tag{3}$$

where $\gamma_{\tilde{n}\tilde{\phi}}$ is the coherence, $\theta_{\tilde{n}\tilde{\phi}}$ is the phase angle between the density and potential fluctuations, and n_{rms} and ϕ_{rms} are the rms values of the fluctuations.

3. RESULTS AND DISCUSSION

Spatial profiles of the edge plasma density and temperature and the plasma floating potential ϕ_f are shown in Fig. 2 for $0.95 < r/\bar{a} < 1.15$. These measurements were made during the steady-state phase of the plasma discharge. The plasma potential ϕ_p may be estimated from the measurements of ϕ_f and T_e as $\phi_p \approx \phi_f + \delta_p T_e$, where δ_p depends on the probe material, the heat load on the probe, the ion species and its temperature, and the secondary electron emission coefficient. Typically, $\delta_p \sim 1$–3 for hydrogen plasmas [11]. Around the LCFS, $r/\bar{a} \approx 1$, the plasma parameters are $n_e = (1\text{–}1.2) \times 10^{12}$ cm^{-3} and $T_e = 30$–40 eV. The characteristic density and temperature scale lengths are $L_n = [-(1/n_e) \times (dn_e/dr)]^{-1} \approx 3$–4 cm and $L_T \approx 2L_n$, respectively. These values are comparable (within a factor of 2) to those for ohmically heated plasmas in TEXT at 2 T [3].

Typical values for the normalized density ($\tilde{n}_e/n_e$) and potential ($\tilde{\phi}_f/T_e$) fluctuations (see Fig. 3 for profiles) around the LCFS are $\tilde{n}_e/n_e \approx 0.05$–0.1 and $\tilde{\phi}_f/T_e \approx 0.1$–0.2, which

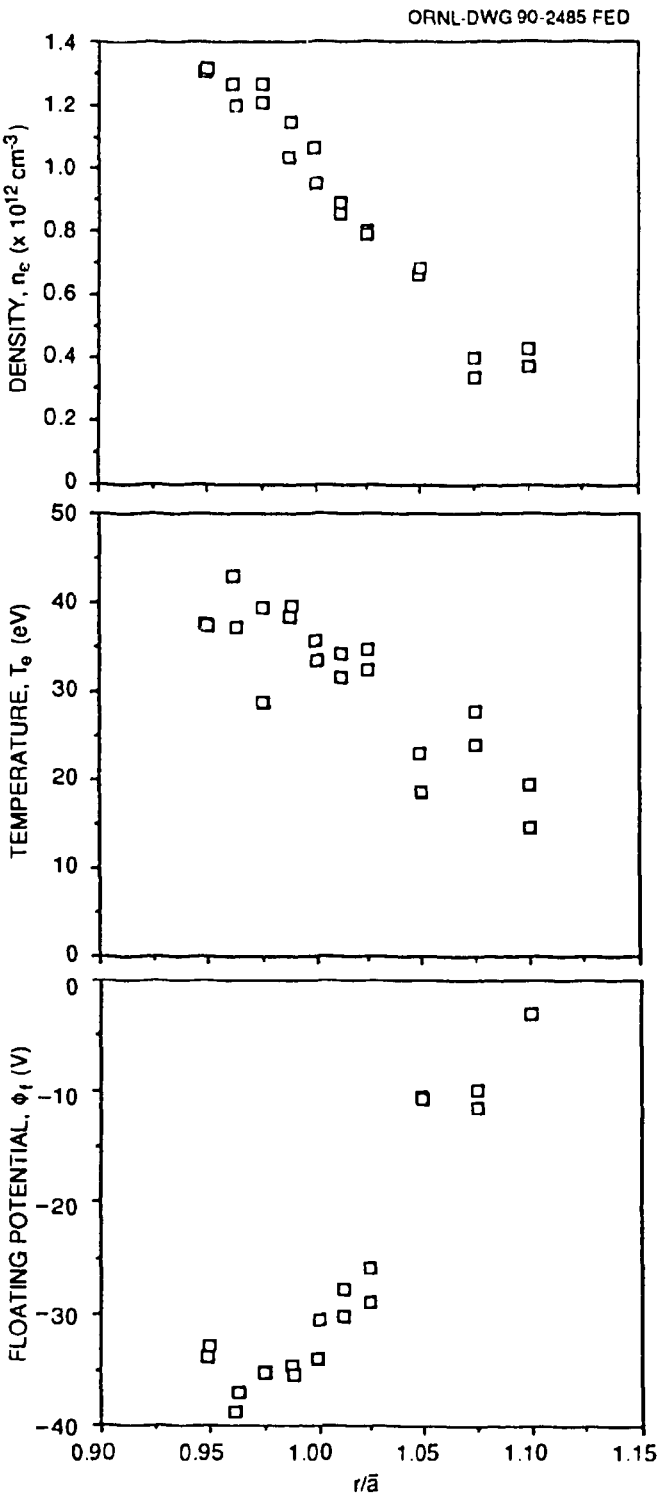

Fig. 2. Spatial profiles of the ATF edge plasma density, temperature, and floating potential.

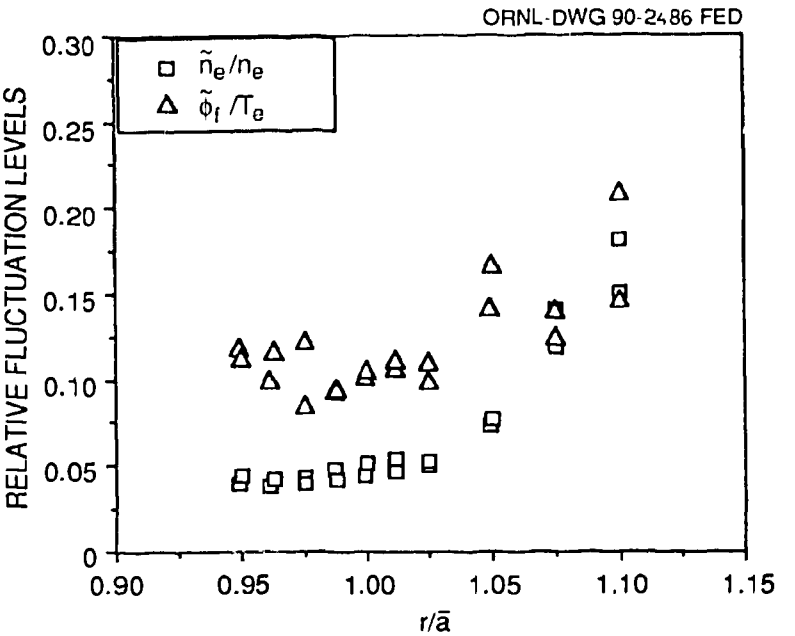

Fig. 3. Relative fluctuation levels for edge density and potential.

are lower than those in TEXT plasmas [3]. Although the correlation between $\tilde{\phi}_f$ and temperature fluctuations $\tilde{T}_e$ in ATF is not yet known, the contribution of $\tilde{T}_e$ to $\tilde{\phi}_p$ has been neglected because the measured values of $\tilde{T}_e$ on TEXT were relatively small ($\tilde{T}_e/T_e \approx 0.4\tilde{n}_e/n_e$) [12]. Fluctuation levels decrease as the probe is moved into the core plasma, where $T_e > 20$ eV and $\tilde{\phi}_f/T_e \approx 2\tilde{n}_e/n_e$ at $r/\bar{a} \approx 0.95$.

Fluctuation spectra of $\tilde{n}_e$ and $\tilde{\phi}_f$ have been examined for frequencies up to 400 kHz. Observed wavenumber-frequency power spectra $S(k,\omega)$ are broadband and mostly in the range 40–300 kHz (as seen in Figs. 4 and 5). The estimated mean value of the wavenumbers from the two probe measurements is $\bar{k} = 1$–3 cm^{-1}, which satisfies $\bar{k}\rho_s \approx 0.05$–$0.1$, where ρ_s is the ion Larmor radius at the sound speed, as observed in TEXT [3]. Analysis of the wavenumber spectra shows that inside the LCFS the spectral width σ_k, the rms deviation about $\bar{k}$, decreases with increasing local electron temperature (Fig. 6), indicating that the correlation length $L_c = 1/\sigma_k$ increases with temperature [13] and typically $L_c \approx 1$ cm, which is much larger than the probe tip separation, for $T_e > 35$ eV. The integrated potential fluctuation power spectra $S(\omega)$ and $S(k)$ decrease for large $\omega/2\pi$ (>200 kHz) and k (as illustrated in Fig. 5) with dependences given by $S(\omega) \sim \omega^{-\alpha}$ and $S(k) \sim k^{-\beta}$, where $\alpha \sim \beta \approx 4 \pm 1$, with a possible deviation from the true shape but a

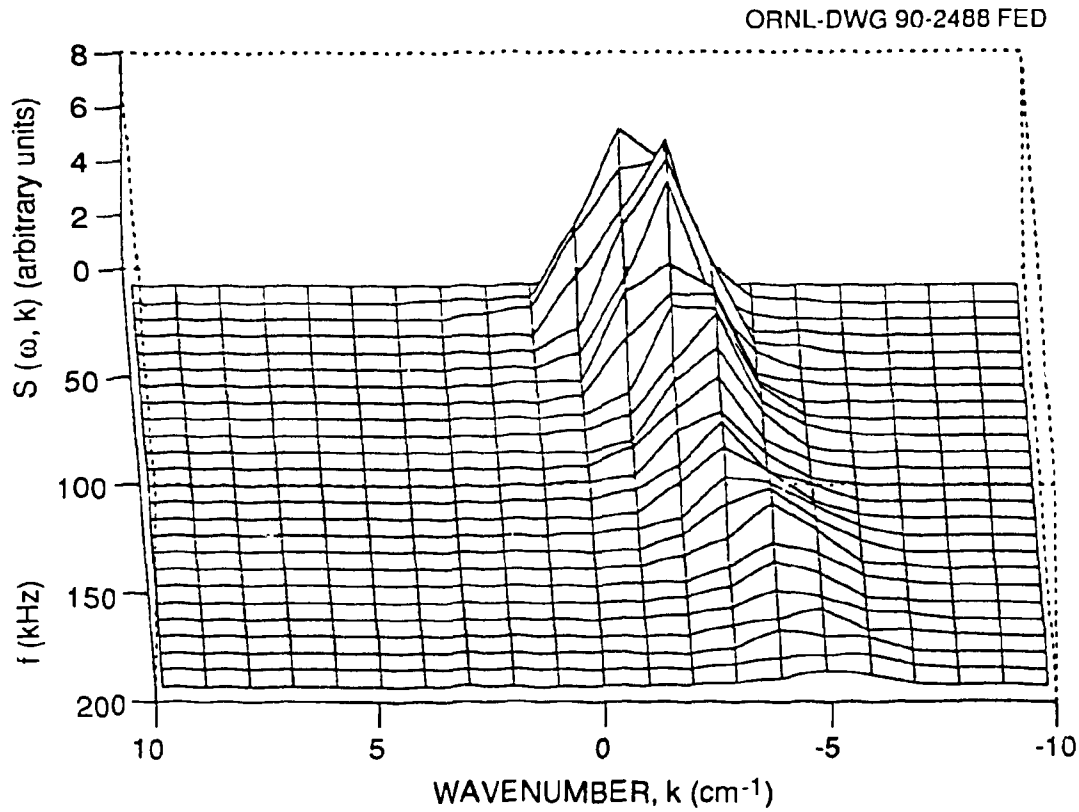

Fig. 4. Wavenumber-frequency power spectrum for potential fluctuations.

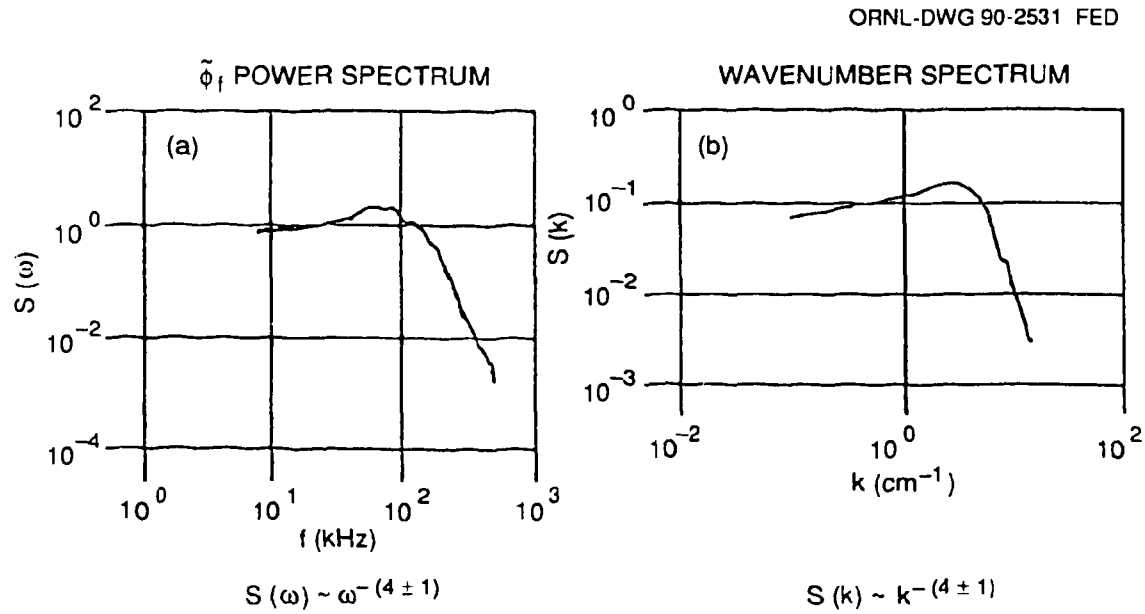

Fig. 5. (a) Power spectrum of the potential fluctuations. (b) Wavenumber spectrum S(k).

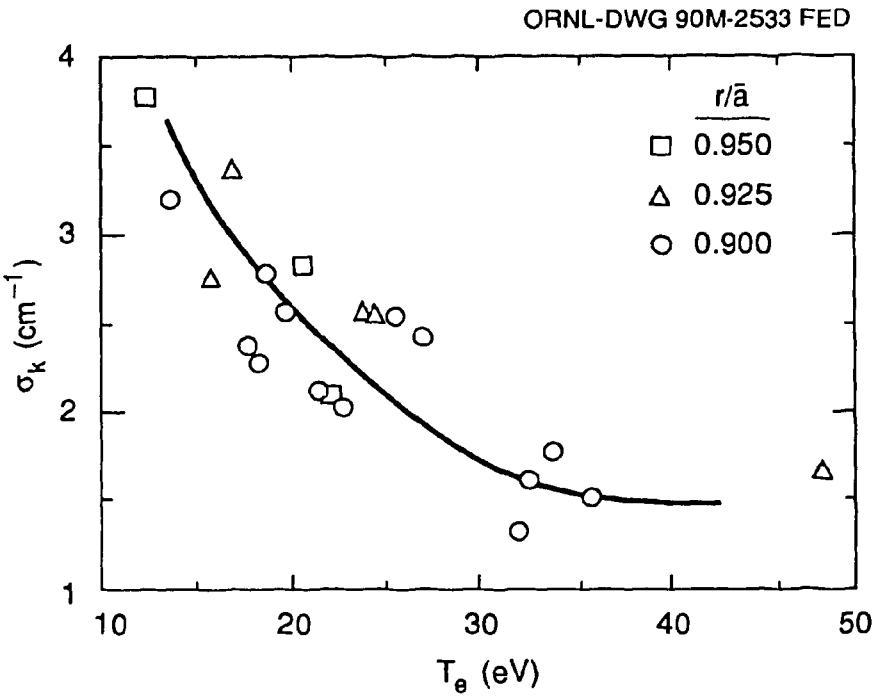

Fig. 6. Variations of σ_k with T_e inside the LCFS.

reliable determination of $\bar{k}$ and σ_k [9,14]. The shape of the $\tilde{n}_e$ spectrum is generally similar to that of $\tilde{\phi}_f$.

The fluctuation-induced particle flux is estimated from Eqs. (1) and (2) by taking $\tilde{\phi}_p \approx \tilde{\phi}_f$. The coherence between the density and the floating potential fluctuations is $\gamma_{\tilde{n}\tilde{\phi}} \approx 0.8$ up to 150 kHz, dropping to ~0.2 beyond 250 kHz, and the corresponding phase angle is $\theta_{\tilde{n}\tilde{\phi}} \approx 70^\circ$ around 150 kHz. The frequency-resolved particle flux $\tilde{\Gamma}(\omega)$ is dominated by frequencies below 250 kHz (Fig. 7) and reaches a maximum at 100–150 kHz, where the phase angle has its maximum. The spatial profile of the total particle flux $\tilde{\Gamma}$, Eq. (1), is given in Fig. 8 for two representative line-averaged densities $\bar{n}_e = 3.5 \times 10^{12}$ cm^{-3} and 5.5×10^{12} cm^{-3}. The radial flux is always outward and at the LCFS has a value $\tilde{\Gamma} \sim 3 \times 10^{15}$ cm^{-2}•s^{-1} for $\bar{n}_e = 3.5 \times 10^{12}$ cm^{-3} and 1.2×10^{15} cm^{-2}•s^{-1} for $\bar{n}_e = 5.5 \times 10^{12}$ cm^{-3}. For the nearly flat core density profiles observed in ATF, the corresponding fluctuation-induced particle confinement times, assuming that $\tilde{\Gamma}$ is constant on flux surfaces, are $\tilde{\tau}_p = (\bar{a}/2)\bar{n}_e/\tilde{\Gamma} \sim 16$ms and 60 ms, respectively. The associated local density diffusion coefficient is $D_n = \tilde{\Gamma}L_n/n_e \sim 1 \times 10^4$ cm^2•s^{-1}, where n_e(edge) ~ 10^{12} cm^{-3} and $L_n \sim 4$ cm for both $\bar{n}_e$ cases. Although detailed scans of $\bar{n}_e$ have not yet been carried out

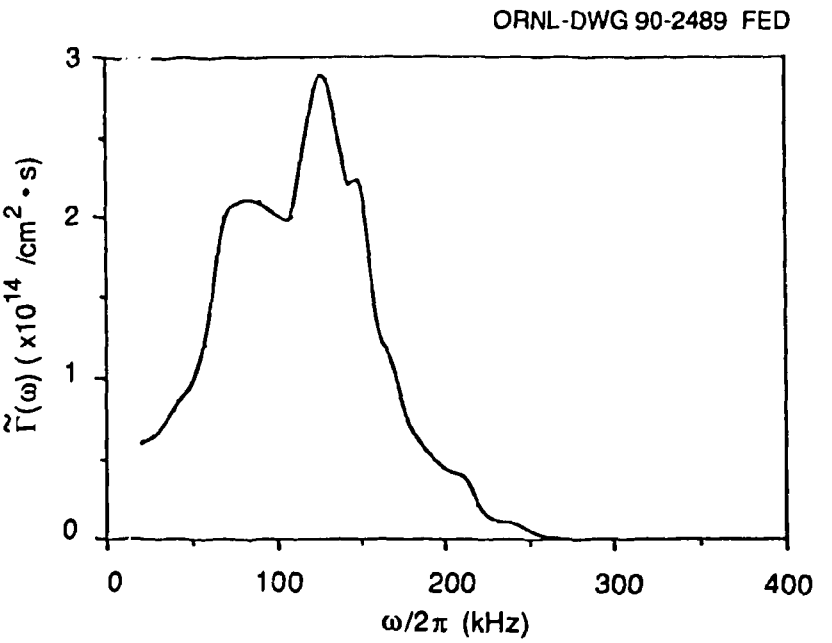

Fig. 7. Typical spectrum of the fluctuation-induced particle flux.

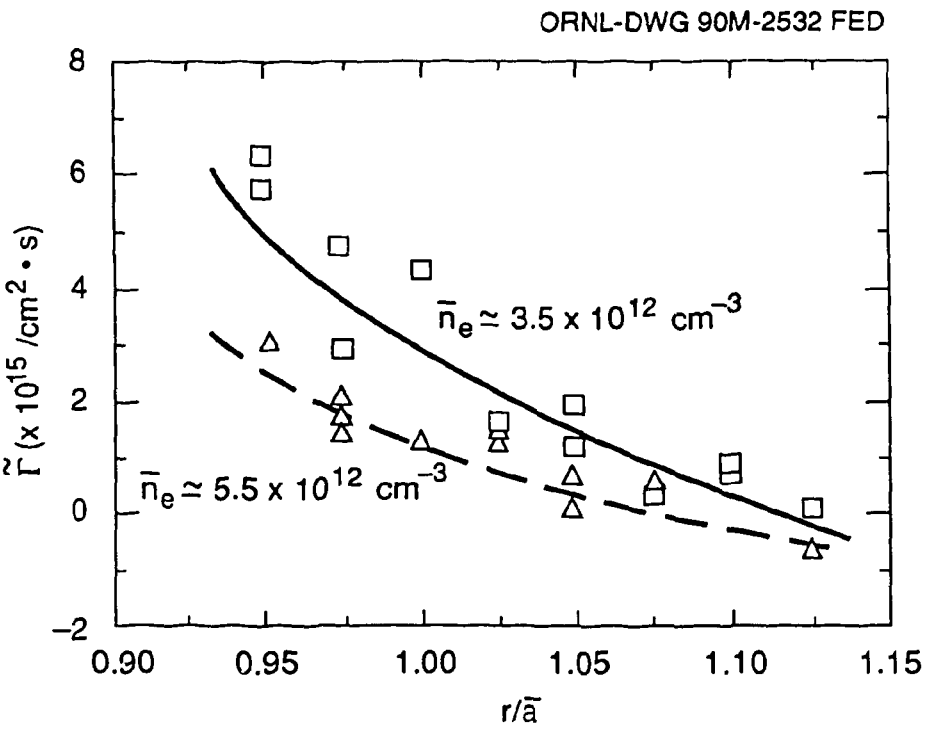

Fig. 8. Spatial profile of the fluctuation-induced particle flux at the edge.

in ATF to determine the scaling of $\tilde{\Gamma}$ with $\bar{n}_e$, results from the present limited scans indicate that τ_p increases with $\bar{n}_e$ in these low-density regime studies. This observation is consistent with the TEXT results [15]. In ATF, it is rather difficult to use H_α spectroscopic measurements for estimating the particle fluxes at the edge because of the lack of a full set of spectroscopic monitors to cover the complicated edge geometry and the existence of particle sources from the divertor stripes around the LCFS [16]. Nonetheless, some comparisons can be made. Based on available data from H_α measurements, the estimated particle flux from the particle balance is $\Gamma_{H_\alpha} \sim (1\text{–}1.5) \times 10^{15}$ cm^{-2}·s^{-1} for $\bar{n}_e = 5.5 \times 10^{12}$ cm^{-3}, which is comparable to $\tilde{\Gamma}$. This suggests that the electrostatic edge turbulence may be responsible for particle confinement characteristics in ATF.

A spatial profile of the mean phase velocity of the fluctuations, $v_{ph} = 2\Sigma_{\omega>0} v_{ph}(\omega)$ with $v_{ph}(\omega) = \Sigma_k(\omega/k)S(k,\omega)/\Sigma_k S(k,\omega)$, is given in Fig. 9. As observed on TEXT [2], the propagation of the fluctuations is in the ion diamagnetic direction for $r/\bar{a} > 1$, but it reverses to the electron diamagnetic direction for $r/\bar{a} < 1$. The location of the v_{ph} shear layer nearly coincides with the peak of the plasma potential where the radial electric field $E_r = -d\phi_p/dr$ changes its direction from outward to inward, as shown in Fig. 10 for $\delta_p \sim 2.5$. At this location, the density and electron temperature gradients are nearly

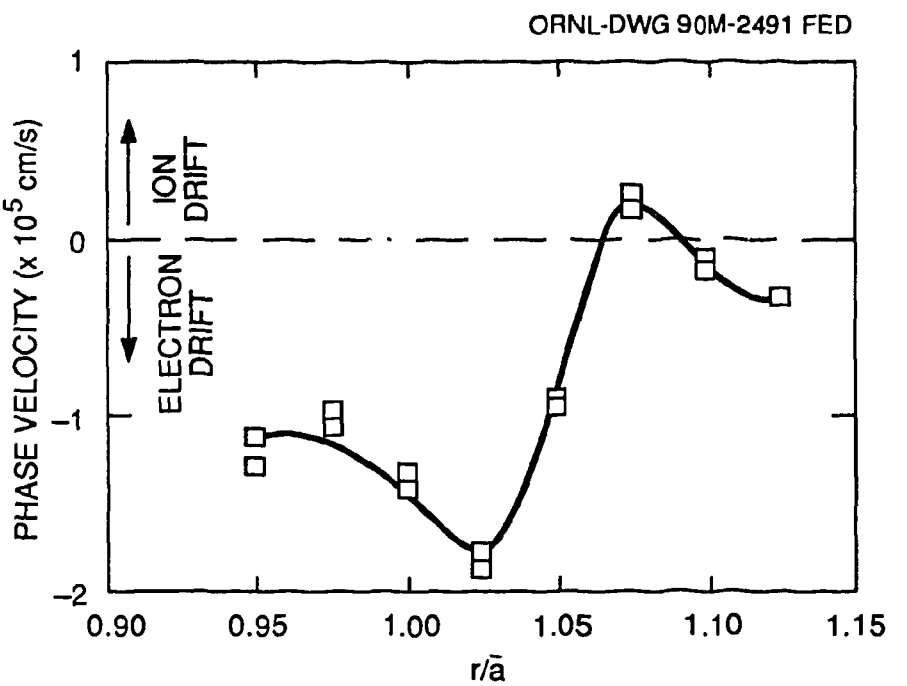

Fig. 9. Spatial profile of the mean phase velocity v_{ph} of the fluctuations. Beyond the shear layer, the wave propagation is in the ion diamagnetic direction.

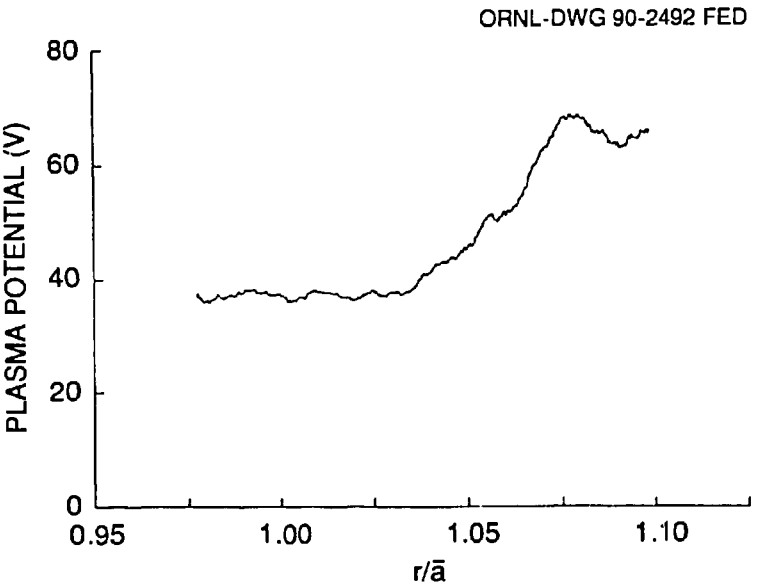

Fig. 10. Spatial profile of the estimated edge plasma potential ϕ_p. The location of the v_{ph} shear layer nearly coincides with the peak of the plasma potential where the radial electric field $E_r = -d\phi_p/dr$ changes its direction from outward to inward.

zero and $v_{ph} \sim v_e \sim 0$, where $v_e = (T_e/eB)(1/L_n + 1/L_T) - E_r/B$ is the electron drift velocity. Also, well inside the LCFS, where $E_r \approx 0$, it is found that $v_{de} \approx v_{ph} \approx 10^3$ m/s.

Future experiments will include measuring the electron temperature fluctuations using the techniques given in refs. [12,17] to determine the relationship between $\tilde{\phi}_p/T_e$ and $\tilde{n}_e/n_e$, scaling of the edge fluctuation parameters with $\bar{n}_e$, and extending the experiments to ECH plasmas with B = 2 T and neutral-beam-heated plasmas. The heavy ion beam probe diagnostic [18] should provide additional information on the plasma potential and its fluctuations.

4. CONCLUSION

The initial results indicate substantial similarities in the characteristics of edge turbulence in the ohmically heated TEXT tokamak and the currentless ATF torsatron. The fluctuation-induced particle flux is consistent with the total particle flux estimated from the global particle balance. Thus, electrostatic turbulence may be responsible for

the edge particle transport. Detailed comparison of the ATF and TEXT results can serve as the basis for development of a unified physics interpretation of edge turbulence in toroidal devices.

ACKNOWLEDGMENTS

The authors thank B. A. Carreras, J. N. Leboeuf, P. H. Diamond, and D. R. Thayer for valuable discussions, M. Murakami and the other members of the ATF group and operating staff for help in carrying out the experiments, and J. Sheffield for continual support and encouragement.

REFERENCES

[1] S. Sudo et al., Nucl. Fusion **30** (1990) 11.

[2] P. Liewer, Nucl. Fusion **15** (1975) 487.

[3] Ch. P. Ritz, R. D. Bengtson, S. J. Levinson, and E. J. Powers, Phys. Fluids **27** (1984) 2956; Ch. P. Ritz et al., Nucl. Fusion 27 (1987) 1125.

[4] J. F. Lyon et al., Fusion Technol. **10** (1986) 179.

[5] Ch. P. Ritz et al., Phys. Rev. Lett. **62** (1989) 1844.

[6] Ch. P. Ritz et al., Rev. Sci. Instrum. **61** (1990) 2998; T. L. Rhodes et al., Rev. Sci. Instrum. **61** (1990) 3001.

[7] T. Uckan et al., Bull. Am. Phys. Soc. **33** (1988) 2069.

[8] E. J. Powers, Nucl. Fusion **14** (1974) 749.

[9] J. M. Beall, Y. C. Kim, and E. J. Powers, J. Appl. Phys. **43** (1982) 3993.

[10] Ch. P. Ritz et al., Rev. Sci. Instrum. **59** (1988) 1739.

[11] P. C. Stangeby, Plasma sheath, in: Physics of Plasma-Wall Interactions in Controlled Fusion, Eds. D. E. Post and R. Behrisch (Plenum, New York, 1986) p. 41.

[12] H. Lin, R. D. Bengtson, and Ch. P. Ritz, Univ. of Texas, Report FRCR-334 (1989).

[13] C. Hidalgo et al., in: Proc. 17th European Conf. Controlled Fusion and Plasma Physics, Amsterdam, 1990 (European Physical Society, 1990), Vol. 14B, p. 1353.

[14] A. Carlson et al., in: Proc. of the Cadarache Workshop on Electrostatic Turbulence, EUR-CEA-FC-1381 (1989), p. 225.

[15] W. L. Rowan et al., Nucl. Fusion **27** (1987) 1105.

[16] P. K. Mioduszewski et al., in: Proc. 16th European Conf. Controlled Fusion and Plasma Physics, Venice, 1989 (European Physical Society, 1989), Vol. 13B, p. 623.

[17] D. C. Robinson and M. G. Rusbridge, Plasma Phys. **11** (1969) 73.

[18] A. Carnevali et al., Rev. Sci. Instrum. **59** (1988) 1670.